

## Quasi-Optic Based HE<sub>11</sub> Miter Bend at 42 GHz for ECRH Application

Amit Patel<sup>1, \*</sup>, Pujita Bhatt<sup>1</sup>, Keyur Mahant<sup>1</sup>, Alpesh Vala<sup>1</sup>, Jitendra Chaudhari<sup>1</sup>,  
Hiren Mewada<sup>3</sup>, and Sathyanarayana<sup>2</sup>

**Abstract**—This paper presents the design and fabrication of HE<sub>11</sub> miter bend along with a TM<sub>11</sub> to HE<sub>11</sub> mode converter and corrugated up-taper, which are the integral parts of a transmission line system (TLS) that carries 200 kW microwave power at 42 GHz from Gyrotron to plasma or calorimetric dummy load. It has a hybrid (HE<sub>11</sub>) mode. The HE<sub>11</sub> mode transmission loss in miter bend is derived using mode-matching techniques and gap loss theory. The gap length ( $L$ ) in a waveguide of diameter ( $D = 2a$ ) at a wavelength ( $\lambda$ ) for the predicted loss ( $D \geq \lambda$ ) is approximately  $1.7[\frac{L\lambda}{2a^2}]^{\frac{3}{2}}$  dB. The HE<sub>11</sub> miter bend design incorporates a demountable cooling assembly with a flat mirror. The design and optimization of the proposed miter bend were carried out using CST-microwave studio software. Finally, HE<sub>11</sub> miter bend was fabricated along with integrated assembly. The proposed HE<sub>11</sub> miter bend with mode converter and corrugated up-taper gives the transmission efficiency of 95.64%.

### 1. INTRODUCTION

In electron cyclotron resonance heating (ECRH) application, gyrotron is mainly used as a high power microwave oscillator [1]. Under the aegis of the Department of Science and Technology (DST — Govt. of India), Institute for Plasma Research (IPR) and other institutes have developed gyrotron at 42 GHz/200 kW that generates power in TE<sub>03</sub> mode [2, 3]. The TE<sub>03</sub> is higher-order and unpolarised mode, which is not suitable for long-distance transmission due to high attenuation (from gyrotron to plasma/dummy load), and plasma heating requires linearly polarized wave. Thus, hybrid (HE<sub>11</sub>) and linearly polarized (LP<sub>11</sub>) modes are the ideal options for this type of application. Therefore, it is necessary to convert TE<sub>03</sub> mode into HE<sub>11</sub> mode. Two methods have been proposed to convert an unpolarized TE<sub>03</sub> mode into polarized HE<sub>11</sub> mode [4–6]. In both the techniques, the HE<sub>11</sub> miter bend is a common integral component which is required for converting the flow of energy from vertical-plane to horizontal-plane (to limit the vertical height of gyrotron TLS).

The loss in the transmission line (TL) depends on the loss of individual components like mode converters, tapers, miter bends, etc. [7]. To reduce it, waveguide transverse dimensions are kept more than the operating wavelength. It kept the ohmic loss of miter bend mirror even smaller at high frequencies [8, 9]. The miter bend is a critical component of TL that contributes to a loss value more than 80% in a total loss. The majority of miter bends have been designed at lower modes like TE<sub>01</sub> mode [10] for circular waveguide and HE<sub>11</sub> mode for overmoded corrugated waveguide [11–13]. Out of the two miter bends, the design and fabrication of HE<sub>11</sub> miter bend are more challenging and costly,

---

Received 30 October 2020, Accepted 24 December 2020, Scheduled 2 January 2021

\* Corresponding author: Amit Patel (amitvpatel.ec@charusat.ac.in).

<sup>1</sup> CHARUSAT Space Research & Technology Center, Chandubhai S Patel Institute of Technology, Charotar University of Science & Technology, Anand, Gujarat 388421, India. <sup>2</sup> Microwave & ECE Diagnostic, Institute for Plasma Research, Gandhinagar, Gujarat, India. <sup>3</sup> Electrical Engineering Department, Prince Mohammad Bin Fahd University, Kingdom of Saudi Arabia.

hence require more precaution. Three techniques have been proposed for the design of  $HE_{11}$  miter bend in the literature [11, 14–17].

The first method contains the phase correction in the mirror of the miter bend. The phase distortion in the incident power creates the mode conversion loss reflected from the mirror of the miter bend that appears at the output of waveguide. In [14], a method is described based on the phase correcting mirror that is suitably contouring these phase errors.

In the second method, the insertion of waveguide taper before the bend increases the waveguide diameter, which reduces the diffraction loss. This method has been suggested in [15, 16] to reduce the mode conversion in miter bend by using up-tapers placed ahead of miter bend which reduces the diffraction. However, it requires large curvatures mirrors, which leads to depolarization and amplitude distortion of the incident field [15, 16].

The third method is based on mode mixtures, which also reduces the diffraction loss [11]. The diffraction loss in miter bend can be reduced by half by extending the grooves up to the mirror of the miter bend [11]. Mode mixtures method has been introduced to reduce diffraction from an open-ended waveguide, for example, in [17] mixtures of  $HE_{11}$  and  $HE_{12}$  with 10% and 20%  $HE_{12}$  have been generated for applications involving coupling of Gaussian beams into corrugated waveguides. In [11], the authors have analysed the mode mixtures of  $HE_{11}$  and  $HE_{12}$  in an appropriate manner, which reduces the diffraction in miter bend using a simple flat mirror without up-tapers. Moreover, the length of mode converter is long (proportional to the beat wavelength), and the diameter of a waveguide is far above the cutoff, making a low loss in a miter bend. As the phase distortion and diffraction loss in miter bend depend on incident power and frequency, it is desirable to add a mode filter that removes the higher-order spurious modes generated from mode converter. They also concluded that when the grooves were not created up to the surface of the mirror,  $HE_{11}$  miter bend made 3% of the total loss, and if it was continued, then the achieved transmission efficiency for pure  $HE_{11}$  mode was more than 99%.

Here, we have proposed a novel model of the  $HE_{11}$  miter bend, which is a hybrid structure of the above techniques. The proposed design of  $HE_{11}$  miter bend contains two overmoded circular corrugated waveguides and one flat mirror along with a demountable water cooling system,  $TM_{11}$  to  $HE_{11}$  mode converter, and corrugated up-taper. The schematic of the proposed model is shown in Figure 1. It is proven that the transmission of high-power at millimetre-wave with low loss is achieved with overmoded circular corrugated waveguide wall [11, 18]. The proposed design is tricky as it incorporates a mode converter on one hand and up-taper on the other hand. Section 2 describes the various losses in  $HE_{11}$

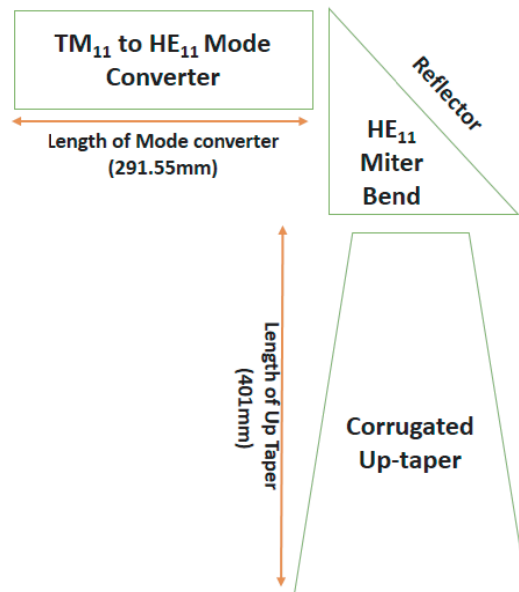


**Figure 1.** Schematic of proposed model.

miter bend. The proposed approach for the  $HE_{11}$  miter bend is illustrated in Section 3 along with its simulation result that has been carried out in CST Microwave Studio software. Section 4 elaborates the fabrication of  $HE_{11}$  miter bend along with its integrated assembly. Finally, the conclusion has been incorporated in Section 5.

## 2. THEORETICAL LOSSES FOR $HE_{11}$ MITER BEND

The predicted loss of miter bend in terms of gap length ( $L$ ) in a waveguide of diameter ( $D = 2a$ ) at a wavelength ( $\lambda$ ) for the predicted loss ( $D \geq \lambda$ ) is given by Equation (1) [11].

$$1.7 \left[ \frac{L\lambda}{2a^2} \right]^{\frac{3}{2}} \quad (1)$$

This loss value comes to approximately 0.5126 dB at an operating frequency 42 GHz and radius as 15.875 mm. The schematic of the predicted loss having gap length ( $L$ ) is shown in Figure 2.

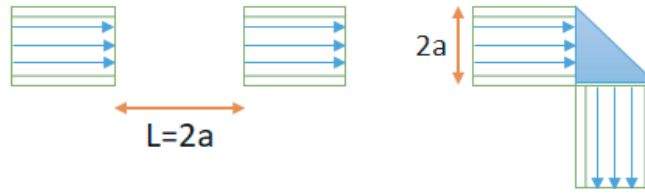


**Figure 2.** Schematic of predicted loss.

The  $HE_{11}$  miter bend theory involves three types of losses: diffraction loss, ohmic loss, and misalignment loss [13, 18]. These losses give the estimation of overall loss before the actual simulation of the component is carried out. The losses are discussed in detail [13]. In a high power transmission line system, the loss of the overall system is highly dependent on the loss of miter bend; therefore, it is necessary to quantify the losses accurately [19].

In this proposed model of  $HE_{11}$  miter bend, the corrugated wall is continued up to the mirror surface, so expected losses are described in Equation (2) [11] where  $L = D$  ( $D = 2a$ ).  $L$  is the distance between the centre of the plane mirror and the exit plane of the  $TM_{11}$  to  $HE_{11}$  mode converter and exit plane of up-taper; ' $D$ ' is the diameter of the waveguide section. This design reduces the loss by a factor two.

$$\text{Diffraction loss} = HE_{11} = 2.4 \left( \frac{\lambda_0}{D} \right)^{\frac{3}{2}} \text{ dB} \quad (2)$$

The theoretical diffraction loss for the  $HE_{11}$  miter bend is  $\sim 0.255$  dB ( $\sim 5\%$ ) as conversion losses encountered in the miter bend design approach.

## 3. PROPOSED DESIGN AND SIMULATION RESULTS

The proposed design of the  $HE_{11}$  miter bend is shown in Figure 3(a). The design incorporates the mode converter  $TM_{11}$  to  $HE_{11}$  (made up of Al-6061T6), support block (Copper), mirror-finished reflector (Copper), and corrugated up-taper (Al-6061T6) to match the corrugated waveguide as shown in Figure 3(a). The magnified portion of the miter bend block is shown in Figure 3(b), indicating grooves on both sides of miter bend, which is due to  $TM_{11}$  to  $HE_{11}$  mode converter and corrugated up-taper.

Direct simulation of  $HE_{11}$  miter bend is not possible in CST Microwave studio software because it does not contain the excitation facility of  $HE_{11}$  mode (85%  $TE_{11}$  and 15%  $TM_{11}$  modes), so  $TM_{11}/TE_{11}$  to  $HE_{11}$  mode converter is required to be designed (here, we have considered  $TM_{11}$  to  $HE_{11}$  mode converter).  $TM_{11}$  to  $HE_{11}$  mode converter has been designed using either linear or nonlinear methods, which were already described in [6]. Both of them have their advantages and disadvantages. The

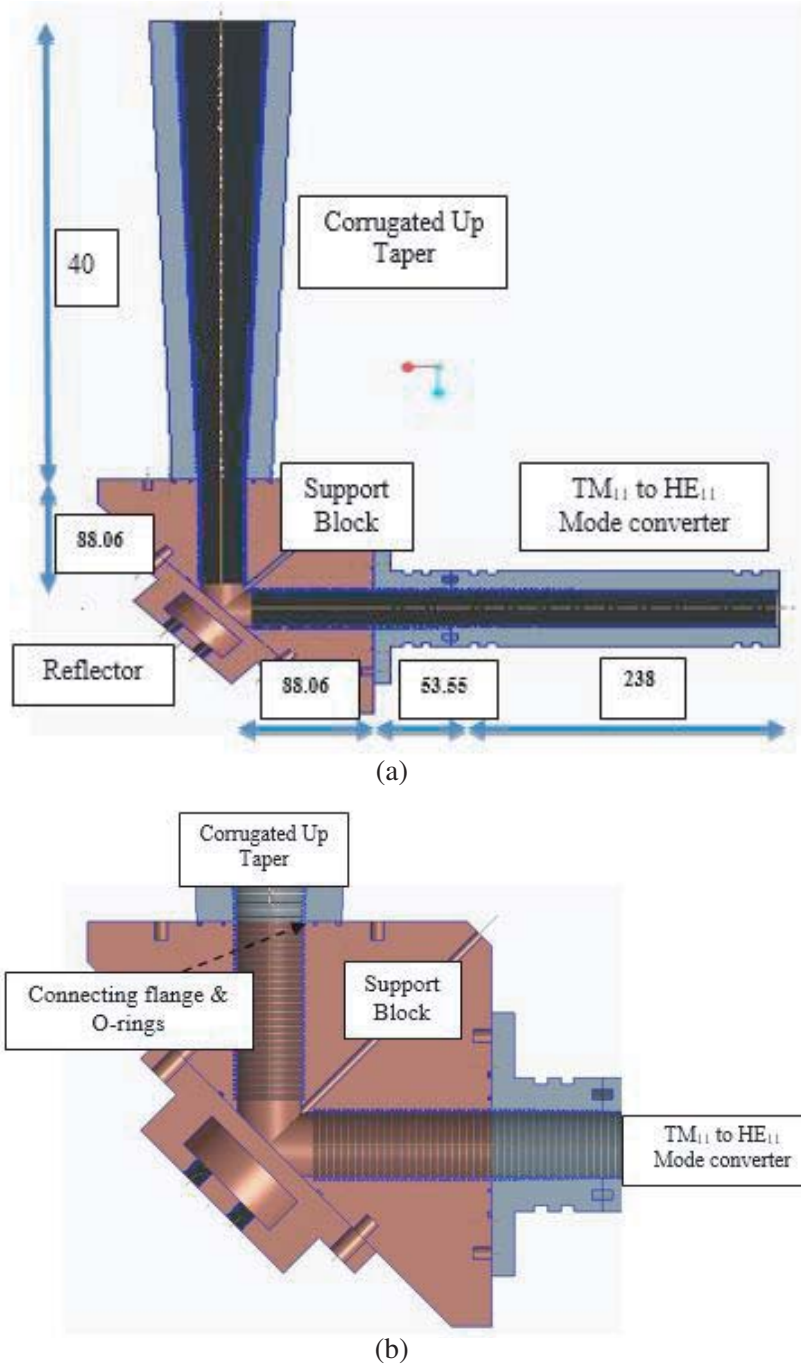


**Figure 3.** (a) Proposed HE<sub>11</sub> miter bend design (All dimensions are in mm). (b) Magnify the part of HE<sub>11</sub> miter bend for better visualization of the internal structure.

nonlinear approach gives a compact structure and high mode conversion efficiency compared to linear method. However, it has manufacturing limitation as it requires accuracy better than 0.1  $\mu\text{m}$ , which is very difficult to achieve and has to pay high manufacturing cost.

On the other hand, the linear technique gives low manufacturing cost because it requires 10  $\mu\text{m}$  accuracy, which can be achieved using a computer numerical controlled (CNC) machine having 8  $\mu\text{m}$  machining accuracy. However, it provides low mode conversion efficiency, and the structure is relatively longer. The proposed TM<sub>11</sub> to HE<sub>11</sub> mode converter has been designed and fabricated in two parts. In

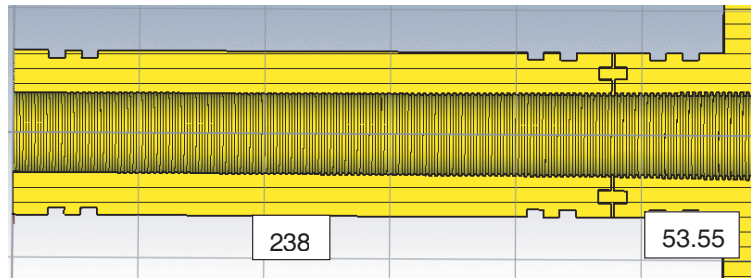


**Figure 4.** The schematic design of  $TM_{11}$  to  $HE_{11}$  mode converter in CST software (All dimensions are in mm).

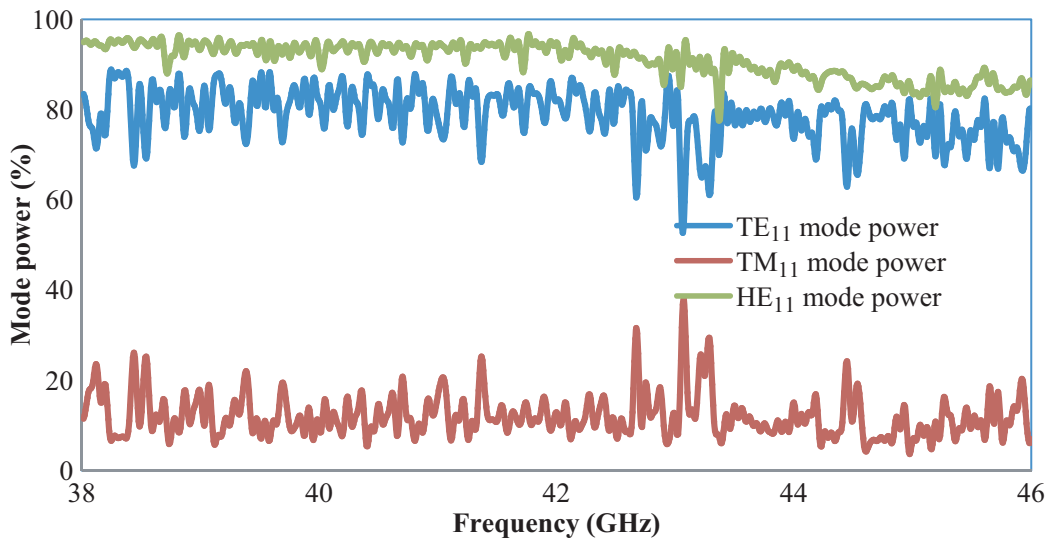


**Figure 5.** Mode power of  $TM_{11}$  to  $HE_{11}$  mode converter.

the first part, the depth of corrugations varies from 0 to  $\frac{\lambda}{8}$  linearly and in the second part varies from  $\frac{\lambda}{8}$  to  $\frac{\lambda}{4}$  non-linearly (to reduce generations of higher-ordered modes). The integrated assembly of both components is shown in Figure 4. The scattering parameters of the proposed mode converter are shown in Figure 5. It represents that the proposed mode converter converts more than 97%  $TM_{11}$  power into  $HE_{11}$  mode. The input and output mode patterns of the mode converter are shown in Figure 6(a) and Figure 6(b).

Similarly, corrugated up-taper is designed to match the diameter of miter bend with corrugated waveguide shown in Figure 7, which carries the power to the plasma or dummy load. The diameter of the corrugated waveguide is 63.5 mm, so we have matched 31.75 mm diameter to 63.5 mm using corrugated up-taper. Like  $HE_{11}$  miter bends, it is not possible to simulate corrugated up-taper in CST Microwave Studio software, so we have connected  $TM_{11}$  to  $HE_{11}$  mode converter to excite  $HE_{11}$  mode.

The return loss of corrugated up-taper is shown in Figure 8 that gives better than 25 dB in operating bandwidth of gyrotron. Figure 9(a) and Figure 9(b) show the input and output mode patterns of corrugated up-taper. The electric field conversion and flow inside the  $TM_{11}$  to  $HE_{11}$  mode exciter and the corrugated up-taper is shown in Figure 10. The output radiation pattern (Gaussian profile of the electric field) of the corrugated up-taper along with the  $TM_{11}$ - $HE_{11}$  mode exciter is shown in Figure 11.

Individual components are optimized and assembled with compatible vacuum O-rings. This design is flexible concerning external flange connections, which can be replaced whenever it is required. The proposed design assembly is simulated using CST Microwave Studio software which is installed in workstation PC Xeon e5-1620V4 having a 96 GB RAM, 2 × 2 TB HDD, and 4 GB GPU with 2 hours battery backup. At 42 GHz, the integrated assembly of  $HE_{11}$  miter bend ( $88.06 \times 88.06 \times 124 \text{ mm}^{-3}$

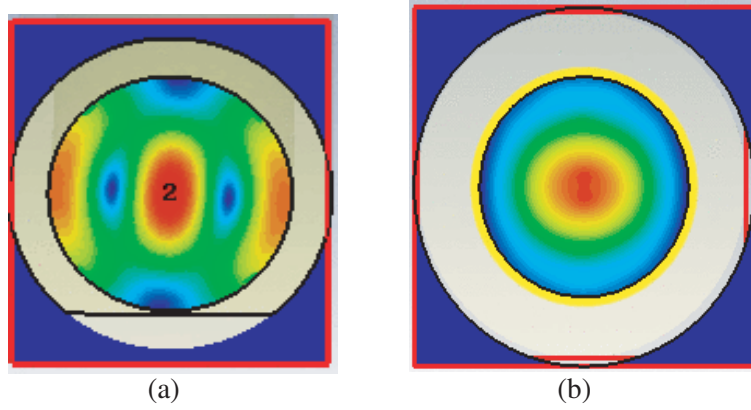


**Figure 6.** (a) Input  $TM_{11}$  mode and (b) output  $HE_{11}$  mode.

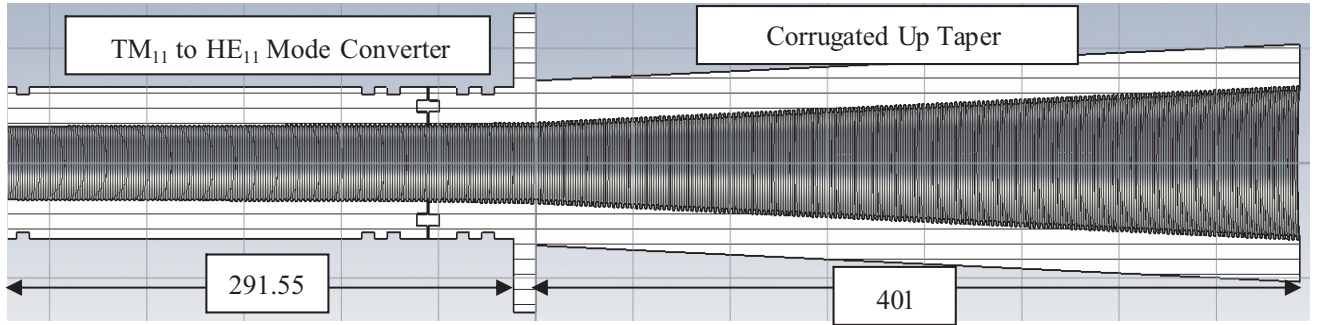


**Figure 7.** Cross-sectional view of the corrugated up-taper along with the  $TM_{11}$ - $HE_{11}$  mode exciter (All the dimensions are in mm).

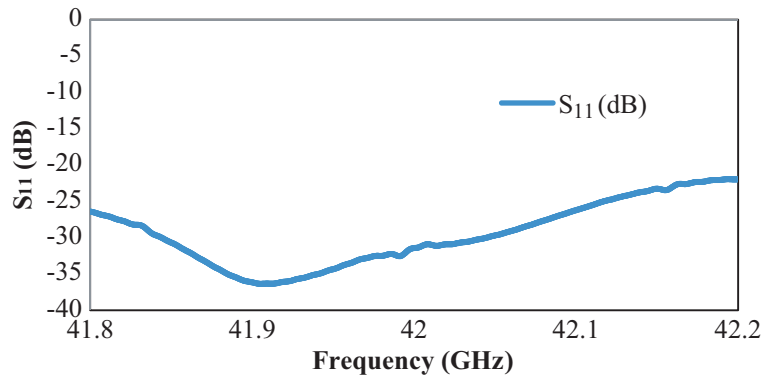


**Figure 8.** Return loss of the corrugated up-taper.

and made-up of copper having  $\rho = 8930 \text{ kg} \cdot \text{m}^{-3}$ ) along with mode converter ( $\phi = 31.75 \text{ mm}$ , length = 294.55 mm, and made-up of aluminium having  $\rho = 3260 \text{ kg} \cdot \text{m}^{-3}$ ) and corrugated up-taper (diameter varies from 31.75 mm to 63.5 mm, length = 401 mm, and made-up of aluminium having  $\rho = 3260 \text{ kg} \cdot \text{m}^{-3}$ ) generated mesh cell 252489933 (at  $\lambda/15$  compared to  $\lambda/20$ , otherwise at  $\lambda/20$  mesh cells became too much large and take more than 1 months for simulation), which took almost 3 weeks for simulation. In the simulation, we have taken the actual dimensions, which are mentioned in Figure 1(a) without any scaling. The scattering parameters of the proposed design are shown in Figure 12, which combines  $TE_{11}$  and  $TM_{11}$  mode contents. The cross-sectional field flow of  $HE_{11}$  miter bend is shown in

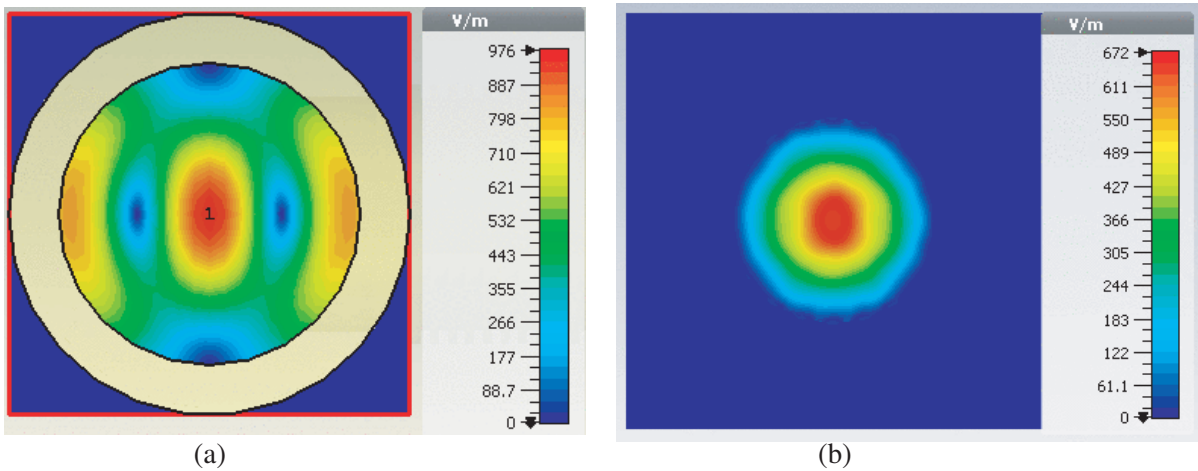


Figure 9. (a)  $TM_{11}$  input and (b)  $HE_{11}$  output mode.

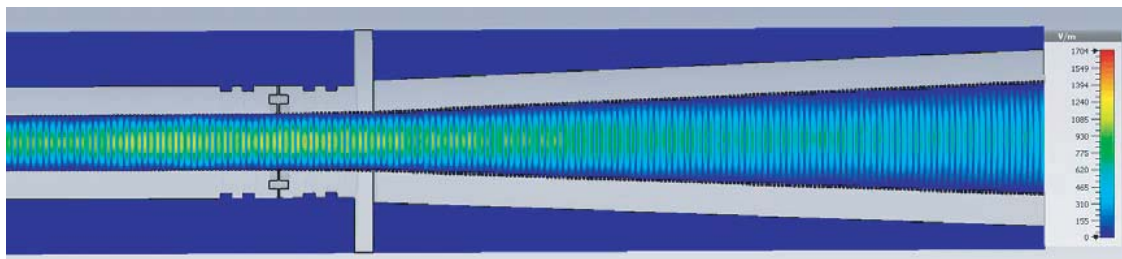


Figure 10. The electric field flow inside the corrugated up-taper.

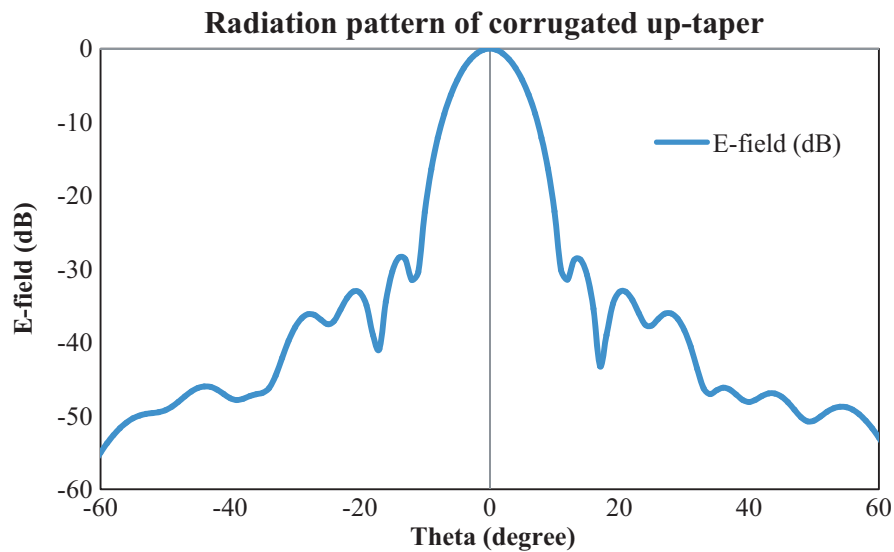
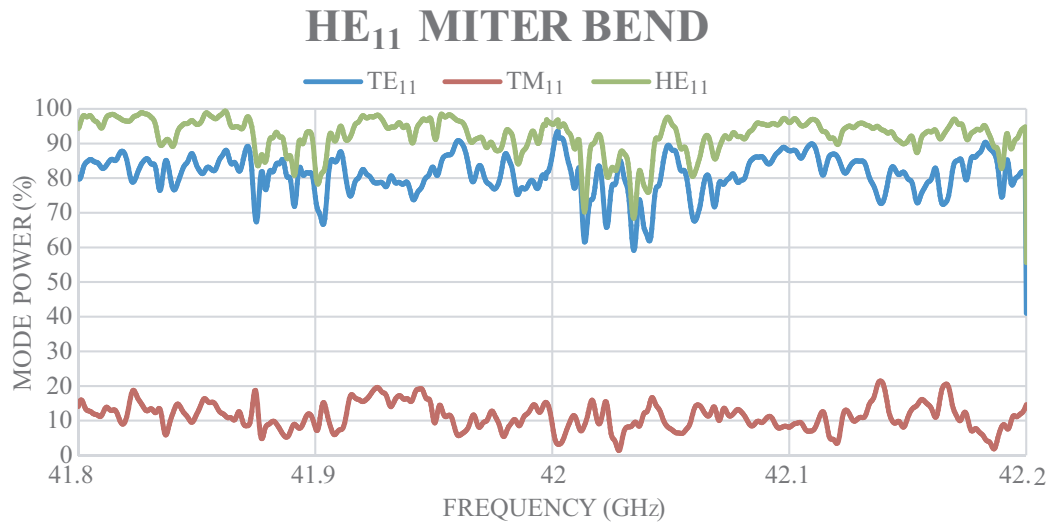
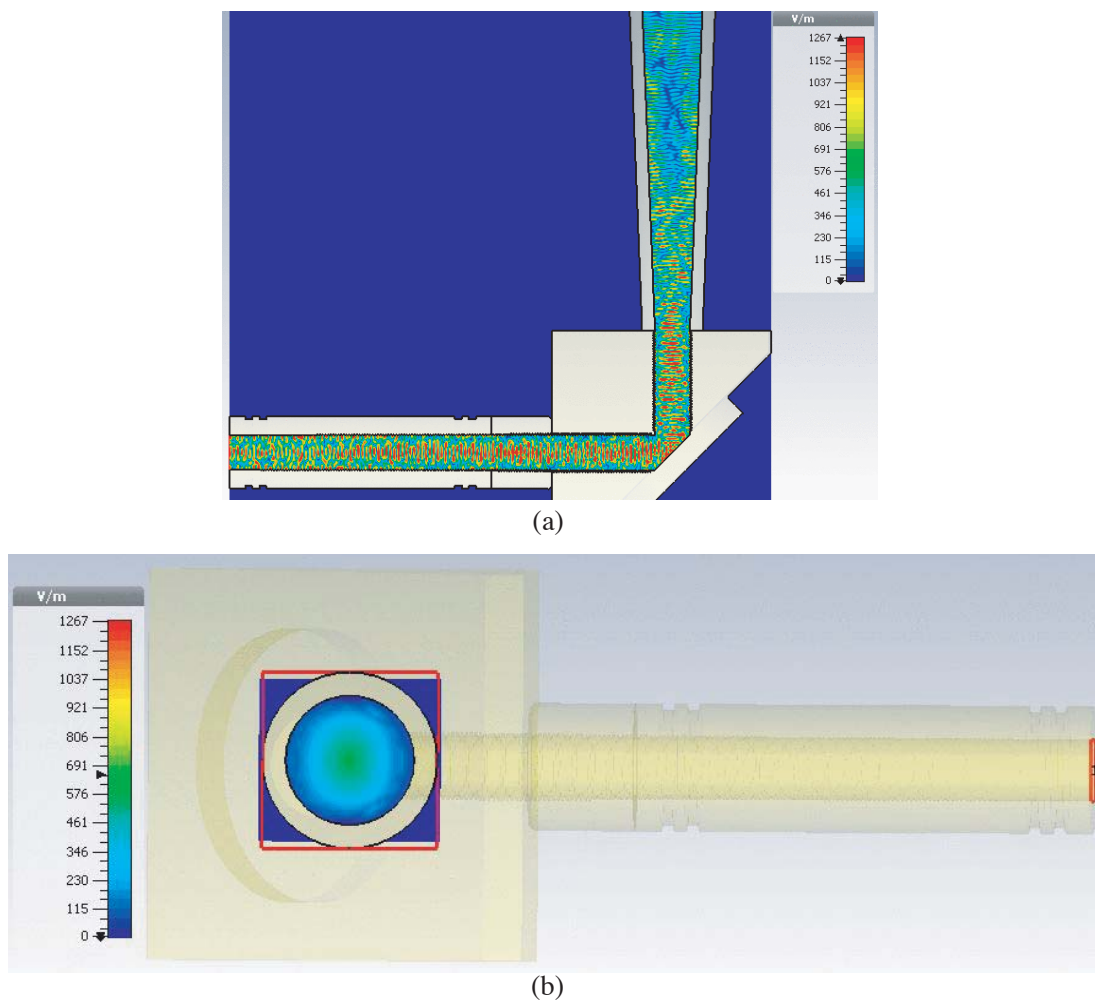


Figure 11. Radiation pattern of the E-field at output of the corrugated up-taper along with the  $TM_{11}$ - $HE_{11}$  mode exciter.

Figure 13(a), and the output mode pattern is shown in Figure 13(b). The theoretical radiation pattern of  $TM_{11}$  and  $HE_{11}$  mode is shown in Figure 14(a), and the corresponding simulated radiation pattern is shown in Figure 14(b).



**Figure 12.** Output mode Power of HE<sub>11</sub> miter bend.



**Figure 13.** (a) Cross-section view of HE<sub>11</sub> miter bend. (b) Output mode of HE<sub>11</sub> miter bend.



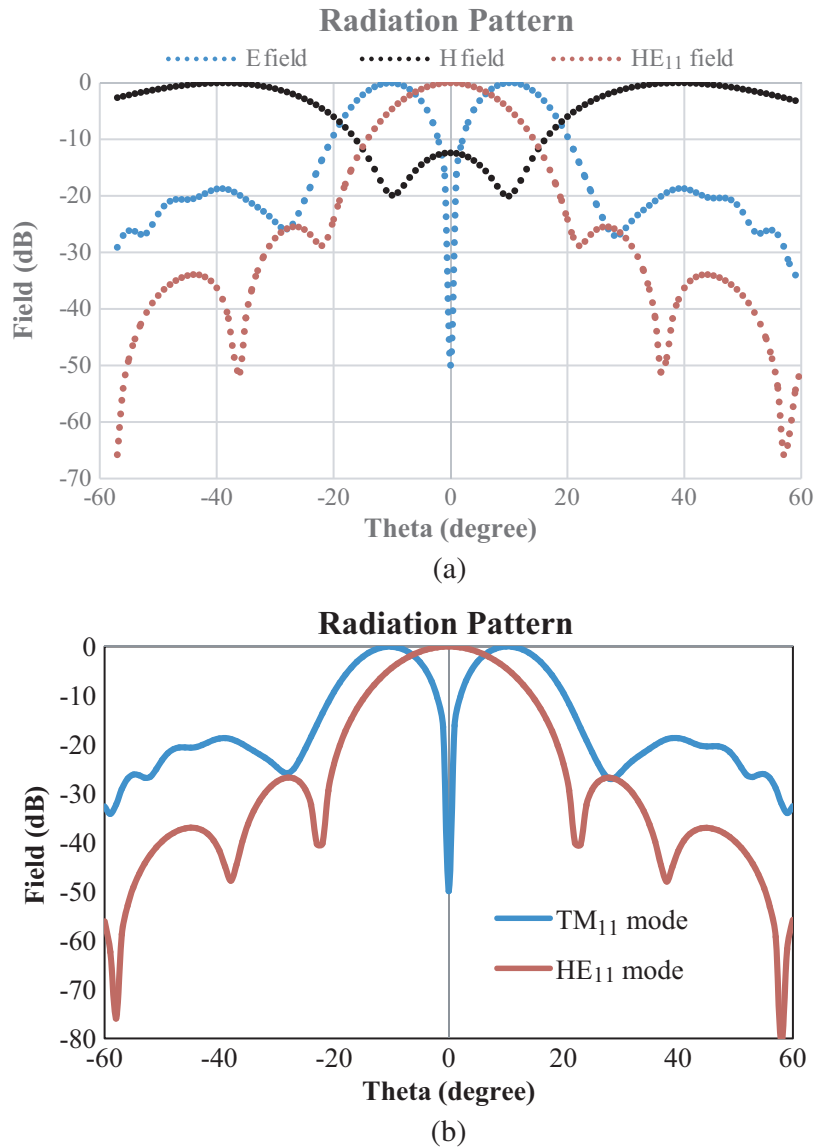


**Figure 14.** Radiation pattern. (a) Theoretical pattern of  $TM_{11}$  mode. (b) Simulated Radiation pattern of HE<sub>11</sub> miter bend.

#### 4. FABRICATION AND TESTING

The manufacturing of HE<sub>11</sub> miter bend along with mode converter and up-taper is quite challenging, hence individual fabrication was carried out. Before actual fabrication, it was necessary to carry out sensitivity analysis of mechanical parameters in terms of microwave performance. The sensitivity analysis was already applied on TE<sub>03</sub> to TE<sub>02</sub> mode converter [20], which concluded that the mechanical tolerance required achieving desired performance was  $\pm 100 \mu\text{m}$ , and it is equally applicable to the proposed design. Hence, the proposed components of HE<sub>11</sub> miter assembly were fabricated along with same mechanical tolerances. A fabricated version of the proposed HE<sub>11</sub> miter bend along with mode converter and up-taper is shown in Figure 15. The schematic of microwave test setup for HE<sub>11</sub> miter bend is as shown in Figure 16. It is tested with the help of vector network analyser ZVA50, and measured results are shown in Figure 17.

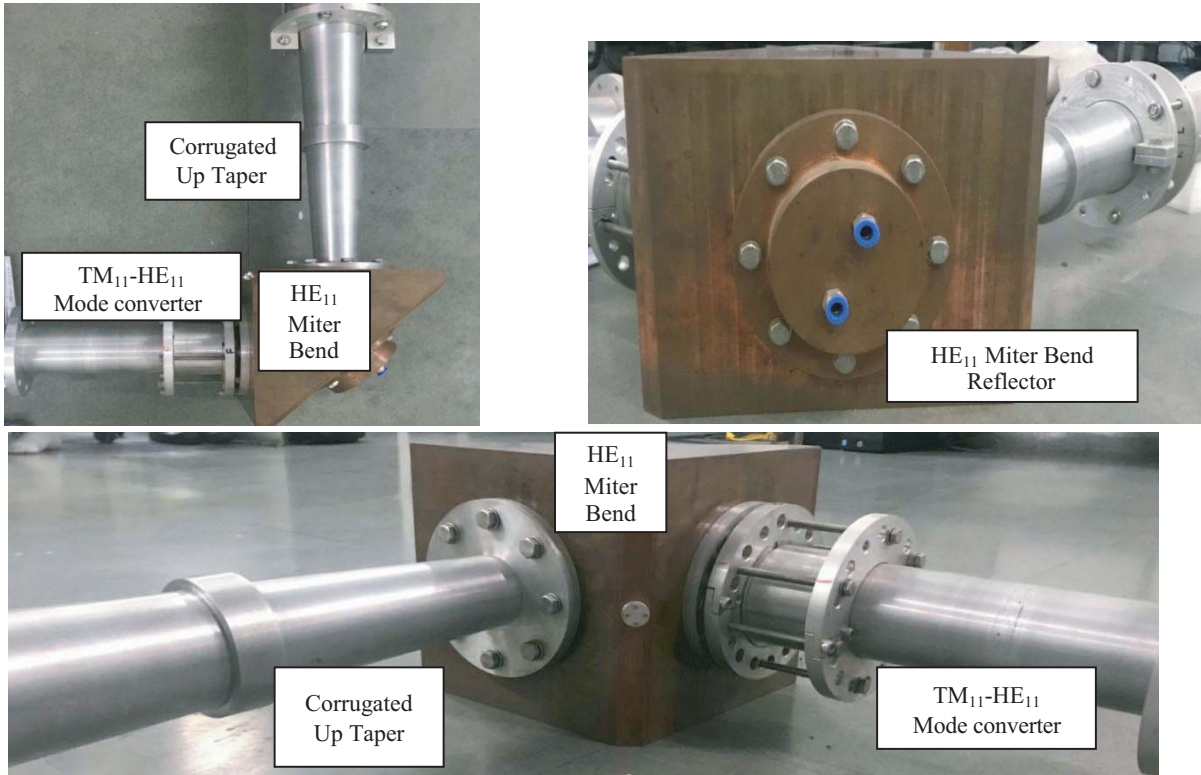


**Figure 15.** Fabricated  $HE_{11}$  miter bend along with  $TM_{11}$ - $HE_{11}$  mode converter, corrugated up-taper, and demountable cooling system.

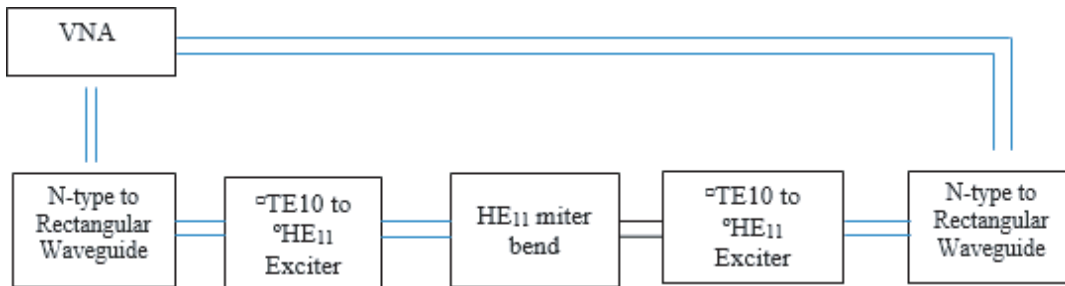


**Figure 16.** Schematic of test set up for  $HE_{11}$  miter bend.

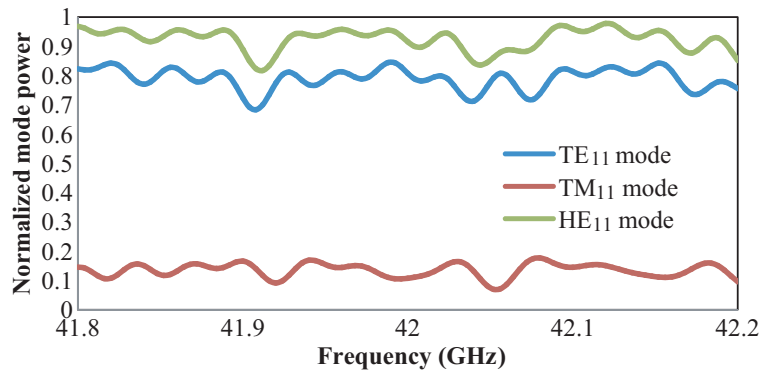


**Figure 17.** Measured result of integrated assembly of  $HE_{11}$  Miter bend.

## 5. CONCLUSION

The design and investigation of  $HE_{11}$  miter bend along with  $TM_{11}$  to  $HE_{11}$  mode converter and corrugated up-taper ( $\phi 31.75$  mm to  $\phi 63.5$  mm) have been proposed in this paper. The internal surface finishing is approximately  $8\ \mu\text{m}$  which is achieved using a CNC machine. It gives low insertion loss and good transmission efficiency within the operating bandwidth of gyrotron ( $42 \pm 0.2$  GHz). The loss generated by  $HE_{11}$  miter bend depends mainly on the purity of  $HE_{11}$  mode that is converted from  $TM_{11}$  mode. For all the pressure and vacuum compatible accessories are mounted on  $HE_{11}$  miter bend for its functional operation. In the end, hands-on experience of the design and fabrication of such a complicated millimetre-wave component are given.

## ACKNOWLEDGMENT

This work is supported by the Board of Research in Nuclear Sciences, Department of Atomic Energy, India [Grant number 39/14/11/2016-BRNS/34196].

## REFERENCES

1. Shapiro, M. A. and S. N. Vlasov, "Study of combined transmission line for high power generates by gyrotron in the mm wavelength range," *International Journal of Electronics*, Vol. 72, 1127–1133, 1992.
2. Singha, U., N. Kumara, H. Khatuna, N. Kumara, V. Yadava, A. Kumara, M. Sharma, M. Alariaa, A. Beraa, P. K. Jain, and A. K. Sinha, "Design of 42 GHz gyrotron for Indian fusion tokamak system," *Fusion Engineering and Design*, Vol. 88, No. 11, 2898–2906, November 2013.
3. Singh, U., U. Goswami, H. Khatun, N. Kumar, N. Shekhawat, A. Kumar, V. Yadav, M. Sharma, A. Mishra, S. Sharma, M. Alaria, A. Bera, R. Rao, and A. Sinha, "Design of 42 GHz, 200 kW gyrotro," *IEEE International Vacuum Electronics Conference, California, USA*, 18–20, May 2010.
4. Thumm, M., "High-power millimetre-wave mode converters in overmoded circular waveguides using periodic wall perturbations," *International Journal of Electronics*, Vol. 57, No. 6, 1225–1246, 1984.
5. Thumm, M., "High power mode conversion for linearly polarized  $HE_{11}$  hybrid mode output," *International Journal of Electronics Theoretical and Experimental*, Vol. 61, No. 6, 1135–1153, 1986.
6. Patel, A., R. Goswami, and P. Bhatt, " $TM_{11}$  to  $HE_{11}$  mode converter in overmoded circular corrugated waveguide," *IET Antenna and Microwave Propagation*, Vol. 3, No. 8, 1202–1207, 2019.
7. Nanni, E. A., S. K. Jawla, M. A. Shapiro, P. P. Woskov, and R. J. Temkin, "Low-loss transmission lines for high-power terahertz radiation," *Journal of Infrared, Millimeter and Terahertz Waves*, Vol. 33, No. 7, 695–714, July 2012.
8. Thumm, M., V. Erckmann, G. Janzen, W. Kasperek, G. Muller, P. G. Schuller, and R. Wilhelm, "Generation of the gaussian like  $HE_{11}$  mode from gyrotron  $TE_{0n}$  mode mixtures at 70 GHz," *International Journal of Infrared and Millimeter Waves*, Vol. 6, No. 6, 459–470, 1985.
9. Tax, D. S., "Mode conversion losses in overmoded millimeter wave transmission lines," Massachusetts Institute of Technology, September 2008.
10. Vikharev, A. A., G. G. Denisov, S. V. Kuzikov, and D. I. Sobolev, "New  $TE_{01}$  waveguide bends," *Journal of Infrared, Millimeter and Terahertz Waves*, Vol. 30, No. 6, 556–565, 2009.
11. Doane, J. L. and C. P. Moeller, " $HE_{11}$  miter bends and gaps in circular corrugated waveguide," *International Journal of Electronics*, Vol. 77, No. 4, 489–509, 1994.
12. Shapiro, M. A. and R. J. Temkin, "High power miter-bend for the next linear collider," *Proceedings of the 1999 Particle Accelerator Conference (Cat. No. 99CH36366)*, Vol. 2, 836–838, IEEE, New York, USA, March 1999.
13. Kowalski, E. J., "Miter bend loss and higher order mode content measurements in overmoded millimeter-wave transmission lines," Ph.D. diss., Massachusetts Institute of Technology, 2010.
14. Vaganov, R. B., "Measurements of losses of certain quasi-optical waveguide elements," *Radio Engineering and Electronic Physics*, Vol. 8, 1228–1231, 1963.

15. Sporleder, F., "A compact  $90^\circ$  corner with expanded diameter and elliptic mirror for circular waveguide," *International Conference on Millimetric Waveguide Systems*, 68–71, London (I.E.E. Conference Publication No. 146), 1976.
16. Vlasov, S. N. and M. A. Shapiro, "Optimization of a miter bend for oversized waveguide with corrugated walls," *Radio Engineering and Electronic Physics*, Vol. 36, 2322–2326 (in Russian issue), 1991.
17. Graubner, T., "Design and measurements of  $HE_{11} + HE_{12}$  mode converters," *17th International Conference on Infrared and Millimeter Waves*, Vol. 1929, International Society for Optics and Photonics, Chengdu, China, 1992.
18. Patel, A., P. Bhatt, K. K. Mahant, A. D. Vala, K. Sathyanarayan, S. V. Kulkarni, and D. Rathi, "Oversized circular corrugated waveguides operated at 42 GHz for ECRH application," *Progress In Electromagnetics Research M*, Vol. 88, 73–82, 2020.
19. Denison, D. R., "Gyrotron mode converter mirror shaping based on phase retrieval from intensity measurement," Massachusetts Institute of Technology, June 1999.
20. Sathyanarayana, K., S. V. Kulkarni, A. Patel, P. Bhatt, A. Vala, H. Mewada, and K. Mahant, "Sensitivity analysis on predicted microwave performance of mode converters with geometrical tolerances for 42-GHz transmission line components," *Fusion Science and Technology*, Vol. 75, No. 3, 234–243, April 2019.